Direct stratigraphic dating of India-Asia collision onset at the Selandian (middle Paleocene, 59 ± 1 Ma)

Xiumian Hu[1]*, Eduardo Garzanti[2], Ted Moore[3], and Isabella Raffi[4]

[1]State Key Laboratory of Mineral Deposit Research, School of Earth Sciences and Engineering, Nanjing University, Nanjing 210023, China

[2]Department of Earth and Environmental Sciences, Università di Milano-Bicocca, 20126 Milan, Italy

[3]Department of Earth and Environmental Sciences, University of Michigan, Ann Arbor, Michigan 48109-1005, USA

[4]Dipartimento di Ingegneria e Geologia, Universita' degli Studi "G. d'Annunzio" di Chieti-Pescara, 66013 Chieti-Pescara, Italy

ABSTRACT

The collision of India with Asia had a profound influence on Cenozoic topography, oceanography, climate, and faunal turnover. However, estimates of the time of the initial collision, when Indian continental crust arrived at the Transhimalayan trench, remain highly controversial. Here we use radiolarian and nannofossil biostratigraphy coupled with detrital zircon geochronology to constrain firmly the time when Asian-derived detritus was first deposited onto India in the classical Sangdanlin section of the central Himalaya, which preserves the best Paleocene stratigraphic record of the distal edge of the Indian continental rise. Deep- sea turbidites of quartzarenite composition and Indian provenance are replaced upsection by turbidites of volcano-plutoniclastic composition and Asian provenance. This sharp transition occurs above abyssal cherts yielding radiolaria of Paleogene radiolarian zones (RP) 4–6 and below abyssal cherts containing radiolaria of zone RP6 and calcareous shales with nannofossils of the Paleocene calcareous nannofossil zone (CNP) 7, constraining the age of collision onset to within the middle Paleocene (Selandian). The youngest U-Pb ages yielded by detrital zircons in the oldest Asia-derived turbidites indicate a maximum depositional age of 58.1 ± 0.9 Ma. Collision onset is thus mutually constrained by biostratigraphy and detrital zircon chronostratigraphy as 59 ± 1 Ma. This age is both more accurate and more precise than those previously obtained from the stratigraphic record of the northwestern Himalaya, and suggests that, within the resolution power of current methods, the India-Asia initial collision took place quasi-synchronously in the western and central Himalaya.

INTRODUCTION

The onset of collision between India and Asia, defined as the moment when Neotethyan oceanic lithosphere was subducted completely at a point along the plate boundary and the two continental margins came into direct contact, terminated a period of very rapid Indo-Asian convergence, and brought about profound consequences on Cenozoic topography, atmospheric circulation, climate, oceanography, and faunal turnover. Defining the age of such major geological event with the best possible accuracy and precision is essential in order to understand its wide paleogeographic consequences and their mutual relationships and feedbacks. How- ever, the range of ages hypothesized by different researchers has remained wide, ranging from as early as the latest Cretaceous (Yi et al., 2011) to as late as the earliest Miocene (van Hinsbergen et al., 2012). Chiefly because of the dearth of suitable stratigraphic sections providing optimal conditions for direct dating, the topic has been debated for decades.

Dating the first arrival and deposition of volcano-plutonic and ultramafic detritus derived from the Asian active margin onto the inner part of the Indian passive margin provides undisputable evidence that collision was well underway and India was welded to Asia in the early Eocene both in the northwestern Himalaya (Garzanti et al., 1987) and southern Tibet (Najman et al., 2010). Unconformities identified at a lower stratigraphic level within the inner Indian mar- gin succession and interpreted as associated with collision onset were dated around the Paleocene- Eocene boundary both in the northwestern and central Himalaya (Garzanti et al., 1987; Li et al., 2015), thus providing an older minimum age for collision onset. Considering the time required by the flexural wave to propagate across the distal Indian margin, collision must have begun some- what earlier, a time that needs to be established from the stratigraphic record of the very distal edge of the Indian continental margin. Distal successions recording the continuous transition from continental rise to trench sedimentation, however, are only exceptionally exposed along the suture zone. The most complete of these is the Sangdanlin section of south Tibet, for which initial collision ages ranging from 50 Ma or earlier (Wang et al., 2011) to ca. 60 Ma (DeCelles et al., 2014; Wu et al., 2014) or even ca. 65 Ma (Ding et al., 2005) were suggested, based principally on detrital zircon geochronology. Here we accurately revise the radiolarian biostratigraphy, calibrated with a new firm nannofossil datum, and provide new detrital zircon U-Pb ages from the crucial interval documenting the sharp provenance change from Indian-derived to Asian-de- rived detritus. The onset of the India-Asia collision could thus be dated directly with improved accuracy and precision.

STRATIGRAPHY OF THE SANGDANLIN SECTION

The Sangdanlin section (29°15’28N”, 85°14’52” E; Fig. 1; Fig. DR1 in the GSA Data Repository[1]) includes three formations. Siliceous shale, chert, and mainly quartzarenitic turbidites of the Denggang Formation are followed by siliceous shale, chert, and interbedded quartzose and volcano-plutonic turbidites of the Sangdanlin Formation, overlain in turn by siliceous shale with thin- to thick-bedded volcano-plutonic turbidites of the Zheya Formation (Fig. 2).

Radiolarian Biostratigraphy

We collected 44 chert samples from the Denggang, Sangdanlin, and Zheya Formations, 28 of which yielded age-diagnostic radiolaria (see methods and Tables DR1 and DR2; see footnote 1), which are not abundant and are poorly preserved. Identifications were based on general outline and size, number of segments (Nassellaria), and pore size, shape, and arrangement when visible (Fig. DR2). Reworking of Cretaceous to Paleocene specimens is common throughout the section (Table DR1). Strati- graphic age was thus based on the earliest appearances of index species.

In units 9–12 (Fig. 2), *Buryella granulata*, *B. foremanae*, *Lithostrobus cf. longus*, and *Orbiculiforma* sp. aff. *renillaeformis* point to Paleogene radiolarian zones RP4–RP6 (Sanfilippo and Nigrini, 1998). In the overlying units 16, 25, and 32, *Bekoma*(?) *demissa*, *Buryella tetradica*, *B. pentadica*, *Calocycloma ampulla*, *Dictyoceras caia*, *Dorcadospyris* sp. *A* (from Blome, 1992), *Lychnocanoma auxilla*, *Phormocyrtis striata exquisita*, and *Theocorys? phyzella* indicate zone RP6 (Sanfilippo and Nigrini, 1998). *Phormocyrtis striata striata* in unit 25 and *Giraffospyris lata* in unit 32 suggest that these strata may extend into zone RP7, although coexistence with *Buryella pentadica* would indicate the uppermost zone RP6 for the lower Zheya Formation (Sanfilippo and Nigrini, 1998; Nishimura, 1992). *Phormocyrtis striata striata* and *Giraffospyris lata* are absent in unit 41, where the radiolarian assemblage resembles otherwise those in units 16, 25, and 32. Zone RP6 ranges from the early Selandian to the early Thanetian (Vandenberghe et al., 2012).

Nannofossil Biostratigraphy

Five mudrock samples from the Zheya Formation were analyzed. Two samples from unit 26 (Fig. 2) yielded a calcareous nannofossil assemblage with moderately preserved specimens including *Biantholithus sparsus*, *Chiasmolithus bidens* gr., *Cruciplacolithus tenuis* s.s., *Ellipso- lithus bollii*, *Ericsonia robusta*, *Fasciculithus clinatus*, *F.* cf. *magnicordis*, *F. tympaniformis*, and *Sphenolithus moriformis* gr. (Fig. DR3 in the Data Repository). This assemblage suggests a biostratigraphic position corresponding to the upper part of Paleocene calcareous nannofossil zone CNP7, constrained between the base of *Fasciculithus tympaniformis* and the base of *Heliolithus cantabriae*, and correlated robustly with the upper part of Chron 26r (Selandian) in Ocean Drilling Program Site 1262 (Agnini et al., 2014).

Detrital Chronostratigraphy

Detrital zircons separated from 3 sandstones in the Sangdanlin Formation (units 14, 15, and 16) yielded 197 concordant U-Pb ages (for analytical details and complete data set, see the Data Repository; Table DR4). These compare well with results of Wang et al. (2011), Wu et al. (2014), and DeCelles et al. (2014), and con- firm provenance from the Asian active margin. The main age cluster is between 103 Ma and 77 Ma (88 grains); the youngest single grain age is 57 ± 1 Ma (Table DR4). The maximum depo- sitional age is constrained to be 58.1 ± 0.9 Ma [weighted mean of 8 grain ages of the youngest cluster (YC) overlapping at 1χρ; YC1χρ(2+) Dickinson and Gehrels, 2009].

AGE OF COLLISION ONSET

The Denggang Formation, characterized by turbiditic quartzarenites fed from the Indian continent and deposited on the Indian continen- tal rise, is capped by quartzolithic basalticlastic turbidites (unit 10). Detrital zircons display the Early Cretaceous (141–117 Ma) U-Pb age peak characteristic of Cretaceous–Paleocene Tethys Himalayan units (Gehrels et al., 2011). A Cretaceous age was inferred previously for the Deng- gang Formation (Wang et al., 2011; DeCelles et al., 2014) because radiolarians in the overlying cherts were assigned to the Campanian (unit 11; Li et al., 2007). However, we show here that radiolarian faunas in units 4–12 belong instead to biozones RP3–RP4 to RP4–RP6, indicating the Danian (Fig. 2). The Denggang Formation is thus reinterpreted to represent the distal equiva- lent of quartzose sandstones generated during the tectonic and magmatic upwelling event that affected northern India in the latest Cretaceous to early Paleocene (Garzanti and Hu, 2015). The overlying red cherts at the base of the Sangdanlin Formation document entirely abyssal and condensed sedimentation during the late Danian and early Selandian, while the distal margin of India was crossing the near-equatorial upwell- ing zone of high biosiliceous productivity (van Hinsbergen et al., 2011). The overlying strata record the crucial transition from quartzose, Indian-derived turbidites (unit 13) to dominantly Asian-derived volcano- plutoniclastic turbidites (unit 14; Fig. 3). Detrital zircons in units 14–16 yielded U-Pb ages mainly between 103 Ma and 57 Ma, documenting continuing magmatism in the Gangdese arc to the north during the Late Cretaceous and Paleocene, and the maximum depositional age of 58.1 ± 0.9 Ma (Fig. DR4; Table DR3). The ra- diolarian assemblage in unit 16 indicates zone RP6. The lower Zheya Formation yielded radiolarian faunas possibly extending to zone RP7 (unit 25) and calcareous nannofossils of upper zone CNP7 (unit 26), constraining deposition firmly to the late Selandian. The top of zone CNP7 was assigned an age of 58.3 Ma by Ag- nini et al. (2014), in excellent agreement with our zircon age data. Paleogene chronostratigraphy, however, is controversial (Westerhold et al., 2012). The top of Chron 26r, corresponding to the Selandian-Thanetian boundary and preceded shortly by the early-late Paleocene event of intense carbonate dissolution, has been recently assigned ages as old as 59.2 Ma (Vandenberghe et al., 2012). A more robust calibration of the magnetostratigraphic scale is thus needed to translate our data into a more precise age for the India-Asia collision onset.

Turbiditic deposition, fed initially from the Indian side only, and next chiefly and finally exclusively from the Asian side, took place at abyssal depths in trench settings. DeCelles et al. (2014) obtained a robust U-Pb zircon age of 58.5 ± 0.6 Ma (2χρ) for a tuff layer at the top of the Zheya Formation (unit 48), which is identical within error to the age indicated by biostratigraphy and zircon chronostratigraphy for the base of the Zheya Formation. This would indicate very rapid accumulation rates (~500 m in less than 1 m.y.), and thus massive turbiditic supply to the trench during the very first collisional stages. However, chert layers of unit 41 in the upper part of the section yielded a radiolarian assemblage similar to that in unit 16, suggesting that they may represent a tec- tonic repetition of the chert interval at the top of the underlying Sangdanlin Formation (Fig. 2). If stratigraphic thickness is duplicated tec- tonically, then accumulation rates do not need to be extreme, and the exposed Asian-derived trench sediments would not be thicker than 300 m and all deposited between the Selandian and the early Thanetian.

REGIONAL EVIDENCE

The onset of collision between India and Asia was first dated stratigraphically in the northwestern Himalaya as ca. 57 Ma, based on the identification of a major unconformity inferred to document uplift associated with the passage over a flexural bulge (Garzanti et al., 1987). Such an age is fully consistent with the age of northwestern Himalayan eclogites dated as 53.3 ± 0.7 Ma, which implies first arrival of Indian continental crust at the Transhimalayan trench ca. 57 Ma (Leech et al., 2005).

A prominent disconformity, marked by a conglomerate packed with clasts eroded from the underlying limestone unit, also occurs within the shallow-water carbonate succession of the inner Indian passive margin in the Gamba section of south Tibet, where it is dated as ca. 56 Ma and equally inferred to document uplift associated with the passage over a flexural bulge (Li et al., 2015). Such a bulge unconformity developed close to the Paleocene-Eocene boundary all along the inner Indian passive margin, ruling out markedly diachronous collision, as suggested independently by Indian foreland-basin succes- sions farther south (Najman et al., 2005).

Our new data indicate that the distal edge of the Indian passive margin reached the Transhimalayan trench in the Selandian (59 ± 1 Ma). Southward propagation of a flexural wave followed during the Thanetian, and reached the inner Indian margin ~3 m.y. after collision onset.

The new detailed biostratigraphic and geochronological data presented in this study tightly constrain the initial collision between the Indian and Asian continents as within the Selandian, without evidence of major diachroneity between the western and central Himalaya. The age of 59 ± 1 Ma is compatible with geological informa- tion retrieved from both the Tethys Himalayan passive margin and the Transhimalayan active margin (i.e., the Cuojiangding section; Fig. 1; Hu et al., 2015), and allows refinement of collision scenarios inferred from paleomagnetic studies of both southern (Yi et al., 2011) and northern margins (Lippert et al., 2014) of the Neotethys Ocean.

CONCLUSIONS

Trench sediments of the Sangdanlin Forma- tion, deposited on top of the subducting Indian plate, document a radical provenance change dated at the middle Paleocene (59 ± 1 Ma) by radiolarian and nannofossil biostratigraphy coupled with zircon chronostratigraphy. The Himalayan orogeny is thus constrained firmly to have begun at least 10 m.y. earlier than inferred previously from the cessation of marine sedimentation in the Tethys Himalaya (e.g., Rowley, 1996).

ACKNOWLEDGMENTS

We thank Juan Li, Jiangang Wang, Wei An, Hui Luo, and Sunlin Chung for their assistance in the field or in the laboratory. This study was financially supported by the Chinese Ministry of Science and Technology (MOST) 973 Project (2012CB822001), the Strategic Priority Research Program (B) of the Chinese Academy of Sciences (XDB03010100), and the National Science Foundation of China (projects 41172092, 40772070). We thank Ellen Thomas, Mary Leech, Chris Hollis, and an anonymous reviewer for their constructive comments.

REFERENCES CITED

Agnini, C., Fornaciari, E., Raffi, I., Catanzariti, R., Pälike, H., Backman, J., and Rio, D., 2014, Biozonation and biochronology of Paleogene calcareous nannofossils from low and middle latitudes: Newsletters on Stratigraphy, v. 47, p. 131–181, doi:10.1127/0078-0421/2014/0042.

Blome, C.D., 1992, Radiolarians from Leg 122, Ex- mouth and Wombat Plateaus, Indian Ocean, *in* von Rad, U., et al., eds., Proceedings of the Ocean Drilling Program: Scientific results, Volume 122: College Station, Texas, Ocean Drilling Program, p. 633–652, doi:10.2973/odp.proc.sr.122.165.1992.

DeCelles, P.G., Kapp, P., Gehrels, G.E., and Ding, L., 2014, Paleocene–Eocene foreland basin evolution in the Himalaya of southern Tibet and Nepal: Implications for the age of initial India-Asia collision: Tectonics, v. 33, p. 824–849, doi:10.1002/2014TC003522.

Dickinson, W.R., and Gehrels, G.E., 2009, Use of U-Pb ages of detrital zircons to infer maximum depositional ages of strata: A test against a Colorado Plateau Mesozoic database: Earth and Planetary Science Letters, v. 288, p. 115–125, doi: 10.1016/j.epsl.2009.09.013.

Ding, L., Kapp, P., and Wan, X.Q., 2005, Paleocene– Eocene record of ophiolite obduction and initial India-Asia collision, south central Tibet: Tectonics, v. 24, TC3001, doi:10.1029/2004TC001729.

Garzanti, E., and Hu, X., 2015, Latest Cretaceous Himalayan tectonics: Obduction, collision or Deccan-related uplift?: Gondwana Research, v. 28, p. 165–178, doi:10.1016/j.gr.2014.03.010.

Garzanti, E., Baud, A., and Mascle, G., 1987, Sedimentary record of the northward flight of India and its collision with Eurasia (Ladakh Himalaya, India): Geodinamica Acta, v. 1, p. 297– 312, doi:10.1080/09853111.1987.11105147.

Gehrels, G., Kapp, P., DeCelles, P., Pullen, A., Blakey, R., Weislogel, A., Ding, L., Guynn, J., Martin, A., and McQuarrie, N., 2011, Detrital zircon geochronology of pre-Tertiary strata in the Tibetan-Himalayan orogen: Tectonics, v. 30, TC5016, doi:10.1029/2011TC002868.

Hu, X., Wang, J., BouDagher-Fadel, M., Garzanti, E., and An, W., 2015, New insights into the timing of the India-Asia collision from the Paleogene Quxia and Jialazi Formations of the Xigaze forearc basin, South Tibet: Gondwana Research, doi:10.1016/j.gr.2015.02.007 (in press).

Leech, M.L., Singh, S., Jain, A.K., Klemperer, S.L., and Manickavasagam, R.M., 2005, The onset of India-Asia continental collision: Early, steep subduction required by the timing of UHP metamorphism in the western Himalaya: Earth and Planetary Science Letters, v. 234, p. 83–97, doi: 10.1016/j.epsl.2005.02.038.

Li, J., Hu, X., Garzanti, E., An, W., and Wang, J., 2015, Paleogene carbonate microfacies and sandstone provenance (Gamba area, South Tibet): Strati- graphic response to initial India-Asia continental collision: Journal of Asian Earth Sciences, v. 104, p. 39–54, doi:10.1016/j.jseaes.2014.10.027.

Li, Y.L., Wang, C.S., Hu, X.M., Bak, M., Wang, J.G., and Chen, L., 2007, Characteristics of early Eocene radiolarian assemblages of the Saga area, southern Tibet and their constraint on the closure history of the Tethys: Chinese Science Bulletin, v. 52, p. 2108–2114, doi:10.1007/s11434-007-0302-1.

Lippert, P.C., van Hinsbergen, D.J.J., and Dupont- Nivet, G., 2014, Early Cretaceous to present latitude of the central proto-Tibetan Plateau: A paleomagnetic synthesis with implications for Cenozoic tectonics, paleogeography, and cli- mate of Asia, in Nie, J., et al., eds., Toward an improved understanding of uplift mechanisms and the elevation history of the Tibetan Plateau: Geological Society of America Special Paper 507, p. 1–21, doi:10.1130/2014.2507(01).

Najman, Y., Carter, A., Oliver, G., and Garzanti, E., 2005, Provenance of Eocene foreland basin sediments, Nepal: Constraints to the timing and diachroneity of early Himalayan orogenesis: Geology, v. 33, p. 309–312, doi:10.1130/G21161.1.

Najman, Y., et al., 2010, Timing of India-Asia collision: Geological, biostratigraphic, and palaeomagnetic constraints: Journal of Geophysical Research, v. 115, B12416, doi:10.1029/2010JB007673.

Nishimura, A., 1992, Paleocene radiolarian biostratigraphy in the northwest Atlantic at Site 384, Leg 43, of the Deep Sea Drilling Project: Micropaleontology, v. 38, p. 317–362, doi:10.2307/1485764.

Rowley, D.B., 1996, Age of initiation of collision between India and Asia: A review of strati- graphic data: Earth and Planetary Science Letters, v. 145, p. 1–13, doi:10.1016/S0012821X (96)00201-4.

Sanfilippo, A., and Nigrini, C., 1998, Code numbers for Cenozoic low latitude radiolarian biostrati- graphic zones and GPTS conversion tables: Marine Micropaleontology, v. 33, p. 109–156, doi:10.1016/S0377-8398(97)00030-3.

Vandenberghe, N., Hilgen, F., and Speijer, R., 2012, The Paleogene Period, *in* Gradstein, F., et al., eds., The geologic time scale 2012: Amsterdam, Elsevier, p. 855–922, doi:10.1016/B978-0-444-59425-9.00028-7.

van Hinsbergen, D.J.J., Steinberger, B., Doubrovine, P.V., and Gassmoller, R., 2011, Acceleration and deceleration of India-Asia convergence since the Cretaceous: Roles of mantle plumes and continental collision: Journal of Geophysical Research, v. 116, B06101, doi:10.1029/ 2010JB008051.

van Hinsbergen, D.J., Lippert, P.C., Dupont-Nivet, G., McQuarrie, N., Doubrovine, P.V., Spakman, W., and Torsvik, T.H., 2012, Greater India Basin hypothesis and a two-stage Cenozoic collision between India and Asia: National Academy of Sciences Proceedings, v. 109, p. 7659–7664, doi:10.1073/pnas.1117262109.

Wang, J., Hu, X., Jansa, L., and Huang, Z., 2011, Provenance of the Upper Cretaceous–Eocene deep-water sandstones in Sangdanlin, south- ern Tibet: Constraints on the timing of initial India-Asia collision: Journal of Geology, v. 119, p. 293–309, doi:10.1086/659145.

Westerhold, T., Röhl, U., and Laskar, J., 2012, Time scale controversy: Accurate orbital calibration of the early Paleogene: Geochemistry, Geophysics, Geosystems, v. 13, Q06015, doi:10.1029/2012GC004096.

Wu, F.-Y., Ji, W.-Q., Wang, J.-G., Liu, C.-Z., Chung, S.-L., and Clift, P.D., 2014, Zircon U–Pb and Hf isotopic constraints on the onset time of India- Asia collision: American Journal of Science, v. 314, p. 548–579, doi:10.2475/02.2014.04.

Yi, Z., Huang, B., Chen, J., Chen, L., and Wang, H., 2011, Paleomagnetism of early Paleogene marine sediments in southern Tibet, China: Implications to onset of the India-Asia collision and size of Greater India: Earth and Planetary Sci- ence Letters, v. 309, p. 153–165, doi:10.1016/j.epsl.2011.07.001.

Manuscript received 8 April 2015 Revised manuscript received 25 July 2015 Manuscript accepted 1 August 2015

Printed in USA

FIGURE CAPTIONS

Figure 1. Simplified geologic map of the Himalaya, showing study area and location of Paleogene sections discussed in text. 1—Sangdanlin; 2—Tingri; 3—Cuojiangding; 4—Zanskar

Figure 2. Biostratigraphy of the Sangdanlin section (Himalaya). The distribution of radiolaria and calcareous nannofossils constrains the age of interbedded Indian- and Asian-derived turbidites within the middle Paleocene (Selandian radiolarian zone RP6 and calcareous nannofossil zone CNP7, respectively). Stratigraphic log after DeCelles et al. (2014); units 1–49 after Wang et al. (2011). Both minimum (after Agnini et al., 2014) and maximum ages (after Vandenberghe et al., 2012; in Ma) are indicated for the lower and upper boundaries of the Selandian stage.

Figure 3. Zircon chronostratigraphy and sandstone petrography of the Denggang and Sangdanlin Formations, Himalaya (including data from Wang et al., 2011; DeCelles et al., 2014). Ternary diagrams: QFL—quartz, feldspar, lithics; LmLvLs—metamorphic lithics, volcanic lithics, sedimentary lithics. The first arrival of Asian-derived turbidites is recorded in middle Paleocene units 14–15, the maximum depositional age of which is constrained by U-Pb ages of detrital zircons of 58.1 ± 0.9 Ma. Triangular diagrams highlight the sharp compositional difference between Indian-derived quartzose turbidites and Asian-derived volcano-plutonic sandstones. Maximum depositional ages of strata inferred from U-Pb zircon chronostratigraphic results obtained in this study, from DeCelles et al. (2014), and from Wu et al. (2014) are compared in the lower panel (five alternative measures of youngest zircon age after Dickinson and Gehrels, 2009).

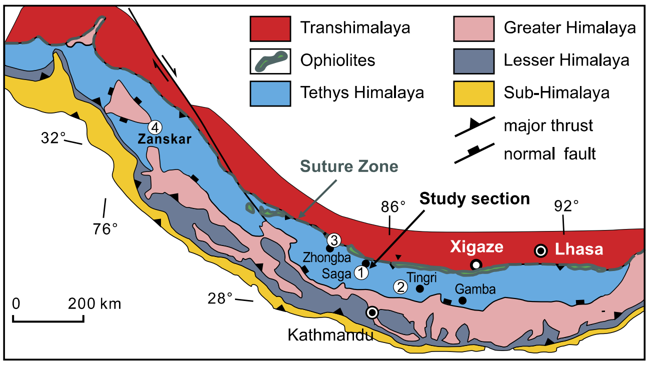

FIGURE 1

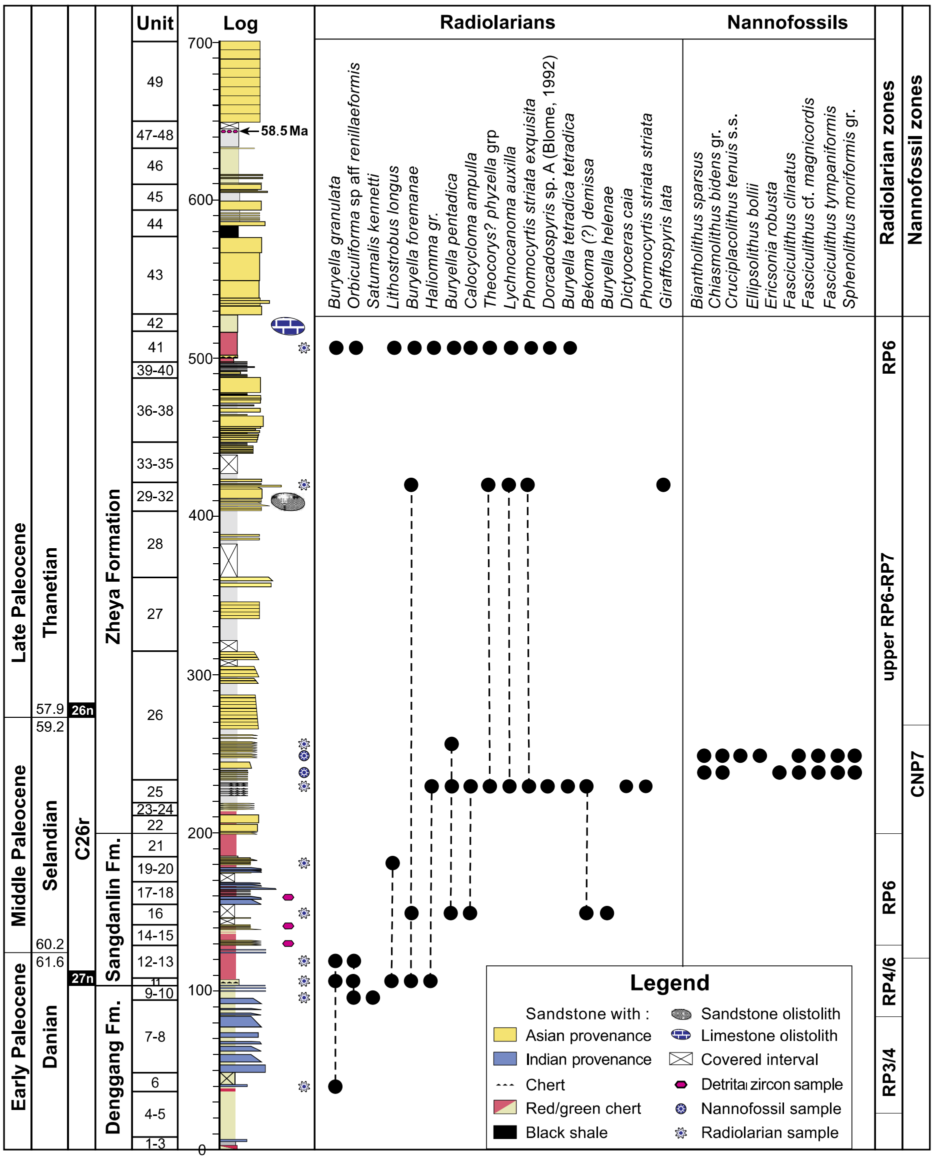

FIGURE 2

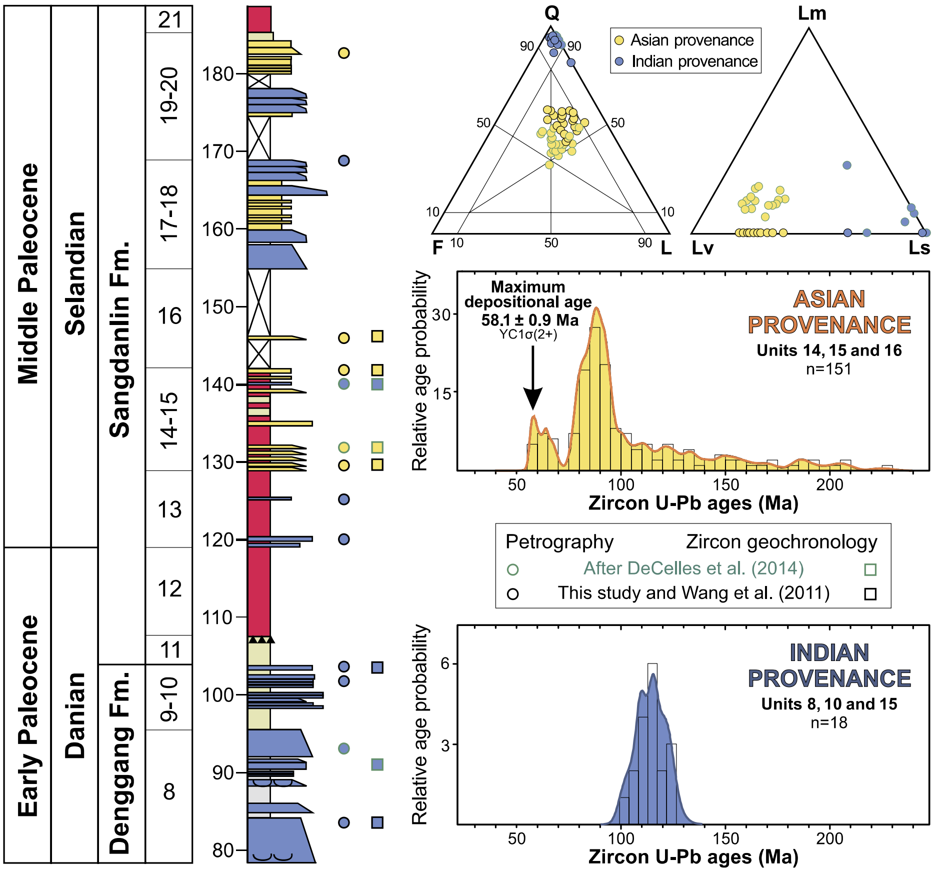

Samples & references	n°	YDZ	YSG	YPP	YC1σ(2+)	n°	YC2σ(3+)	n°
06SDL14/15/16 (this study)	197	56.2+1.5/-3.1	57±1	58.5	58.1±0.9	8	58.6±1.2	11
1SA131 (DeCelles et al. 2014)	97	55.8+4.5/-18	58±9	60.3	60.4±3.2	6	66.0±7.0	11
SDL05/08/09 (Wu et al. 2014)	356	56.2+3.5/-15	57±2	62	58.0±2.8	2	61.2±1.9	8

FIGURE 3